REMARKS

Favorable reconsideration is respectfully requested in view of the foregoing amendments and the following remarks.

Applicants sincerely thank the Examiner for conducting an interview with Applicants' representative.

I.   CLAIM STATUS AND AMENDMENTS

Claims 1 and 4 were pending in this application upon filing of the Preliminary Amendment with the RCE on July 22, 2008. Claims 1 and 4 were indicated as rejected in the Advisory Action mailed June 18, 2008.

Claims 1 and 4 are amended to clarify the claimed invention.

Support for "simultaneously" in amended claims 1 and 4 can be found throughout the specification. In particular, Applicants note that page 8, paragraph [0042] indicates concurrent passing of the specimen molecule solution and the probe molecule solution. Also, paragraph [0059] on page 11 indicates that the present invention is directed towards introducing a probe-containing solution and a specimen-containing solution intro a micro flow channel as laminar flows and measuring the degree of diffusion. Applicants note that no diffusion can occur if the two solutions are not passed through the micro channel at the same time. Further support can be found in paragraph [0013] on page 3 and paragraph [0025] on page 5.

Support for "wherein diffusion of solutes in the solutions is accelerated by affinity between the fluorescent probe molecules and the specimen molecules to form complexes" can be found in paragraph [0025] on page 5. All other amendments to these claims are merely made for clarification purposes.

Thus, no new matter has been added.

II.   ANTICIPATION/OBVIOUSNESS REJECTIONS

In the Office Action dated February 22, 2008, claims 1 and 4 were rejected under 35 U.S.C. § 102(b) as anticipated by Wolinsky et al. Further, claims 1 and 4 were rejected under 35 U.S.C. § 103(a) as obvious over Wolinsky et al. in view of Chee et al.

Applicants respectfully traverse these rejections as applied to the amended claims for the following reasons and for the reasons of record.

4

Applicants note that the claims 1 and 4 are directed towards method for quantitative determination or analysis comprising <u>simultaneously</u> passing a solution containing a specimen molecule and a separate solution containing a fluorescent probe molecule capable of forming a complex with the specimen molecule through a micro flow channel such that laminar flows are formed. As is clear from the amended claim language and specification, the claimed methods require at least two simultaneous laminar flows in the microflow channel to measure changes in diffusion due to affinity between the specimen molecules and fluorescent probes. On the other hand, the primary reference is directed towards, in part, fluorescence activated flow cytometry. In flow cytometry, the specimen and fluorescent probes are mixed prior to flow through a micro flow channel and thus fail to teach each and every element of this claim. Furthermore, the calibration curve in fluorescent flow cytometry is used to calibrate the machine <u>not</u> to quantitatively analyze the specimen molecules. A person of skill in the art reading the claims in light of the specification would easily understand that the calibration curve of the claimed invention is used to determine the amount of specimen molecule in the specimen molecule solution. A person of skill in the art would further understand that this calibration curve is fundamentally different than the calibration curve taught in Wolinsky et al. Applicants note that under US practice the claims are read in light of the specification. Thus, the calibration curve of the amended claims, as read in light of the specification, is not the same as the calibration curve of the cited references.

Thus, for the above-noted reasons, these rejections as applied to the amended claims are untenable and should be withdrawn.

Furthermore, Applicants provide the following remarks:

Wolinsky et al. requires a fluorescence activated flow cytometry in step e) of Claim 1. In flow cytometry, the hybridization procedure is first undertaken usually to prepare a fluid dispersion in order to form complexes between the specimen molecules and the probe molecules immobilized on beads as a solid-phase carrier and then the fluid dispersion is passed through a micro flow channel to make up a laminar flow in which orientation of the complexes is effected for laser measurement. For further information on the flow cytometry, please see Attachment A (Basic Flow Cytometry).

In this way, it is necessary in Wolinsky et al. to perform hybridization of specimen molecules as a pretreatment.

5

As described in paragraph [0007] of the specification, however, a quantitative analysis using a solid-phase carrier with high precision requires strict control of the probe molecules to be immobilized on the solid-phase carrier and, such a control is unavoidably under limitation due to non-uniformity of the efficiency of immobilization of the probe molecules on the solid-phase carrier, poor reproducibility, complicated nature of the surface diffusion behavior of the materials on the solid-liquid interface, and insufficient skill of the workers in conducting the interaction of the specimen molecules.

Furthermore, as shown in [0030] of the specification, the "solution hybridization" on page 12 of Wolinsky et al. and Chee et al., has to be carried out under strict temperature and concentration controls, and thus requires a high-level skill for the laboratory workers. For further information, please see Attachment B (Molecular Cloning).

Accordingly, the method of the claimed invention has been completed with an object to exclude any uncertainty in the analytical results due to differences in the skillfulness of the laboratory workers with respect to complex formation between probe molecules and specimen molecules.

In this way, the claimed invention has been completed with an object to overcome the aforementioned defects possessed by flow cytometry disclosed in Wolinsky et al. Accordingly, the claimed method is neither taught nor suggested by Wolinsky et al. Thus, these rejections are untenable and should be withdrawn.

Attachment C illustrates the difference between the present method and conventional flow cytometry. The right side of this figure shows conventional flow cytometry wherein hybridization is first undertaken as a pretreatment to form a complex between the specimen molecules and the probe molecules immobilized on solid-phase carriers followed by injection of the complex into a micro flow channel. In contrast thereto, the left side of this figure shows the method of the present invention wherein the specimen molecules and probe molecules are separately injected into a micro flow channel so as to form a complex in the micro flow channel.

The Examiner asserted in the Advisory Action that, since the claims read as passing a single solution containing (1) specimen molecules and a (2) solution containing fluorescent probe molecules through the micro flow channel, the claims do not preclude pre-mixing such as hybridization.

Applicants have amended claims 1 and 4 to clarify the claimed invention and avoid misunderstanding.

The Examiner asserted in the Final Rejection that, since Chee et al. teaches quantitation of nucleic acids based on the signals generated by the sample of interest that is then compared to a calibration curve to measure the concentration of the analyte (column 58, lines 25-40), the skilled artisan would have been motivated to combine the teachings of Wolinsky et al. and Chee et al.

However, on conventional flow cytometry, <u>it is impossible to conduct analysis by detecting the changes in the degree of diffusion as in the claimed invention since the molecules are immobilized onto a solid-phase carrier and therefore cannot diffuse.</u> On page 13 of Wolinsky et al., "Three-Color Analysis of Cell Surface Markers" describes that the analysis is made by comparison of the color tone obtained by flow cytometry with the color tone of the sample.

Thus, for the above-noted reasons, these rejections are untenable and should be withdrawn.

III. PROVISIONAL OBVIOUSNESS-TYPE DOUBLE PATENTING REJECTION

In the previous Office Action, claims 1 and 4 were provisionally rejected on the grounds of non-statutory obviousness-type double patenting over claims 1 and 3 of co-pending application number 10/527,987 in further view of Chee et al.

This application has been abandoned and therefore this rejection is moot.

IV. FURTHER REMARKS

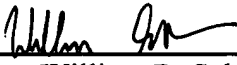Attached herewith is an article by Yamaguchi et al. (Attachment D) to aid the Examiner's understanding.

CONCLUSION

In view of the foregoing amendments and remarks, it is respectfully submitted that the present application is in condition for allowance and early notice to that effect is hereby requested.

If the Examiner has any comments or proposals for expediting prosecution, please contact the undersigned attorney at the telephone number below.

Respectfully submitted,

Kenichi YAMASHITA et al.

By: _____
William R. Schmidt, II
Registration No. 58,327
Attorney for Applicants

WRS/lc
Washington, D.C. 20006-1021
Telephone (202) 721-8200
Facsimile (202) 721-8250
October 30, 2008

ATTAHCMENTS

A. "Basic Flow Cytometry." <http://flowcytometry.med.unc.edu/basicflow.htm.> September 24, 2008.

B. "Synthetic Oligonucleotide Probes." Molecular Cloning. Second Edition.

C. Diagram contrasting claimed invention and conventional flow cytometry.

D. Yamaguchi, Y. et al., "3-D Simulation and Visualization of Laminar Flow in a Microchannel with Hair-Pin Curves", AIChE Journal, (2004), 50(7): 1530-1535.

BASIC FLOW CYTOMETRY

Overview – Flow cytometry is a powerful technology for investigating many aspects of cell biology and for isolating cells of interest. Flow cytometry utilizes highly focused, extremely bright beams of light (usually from lasers) to directly reveal aspects of cells – e.g size and granularity – by the way light is scattered or indirectly by attaching fluorescent probes to cell components e.g DNA binding dyes or labeled antibodies. The power of flow cytometry derives from the fact that it quantitatively analyzes individual cells, thus permitting the identification of subpopulations within a sample. The power of single cell analysis is compounded by the ability to measure multiple parameters simultaneously on each individual cell, to do this very fast (in excess of 20,000 cells/second), and to isolate/purify/sort desired subpopulations (up to 4 simultaneously).
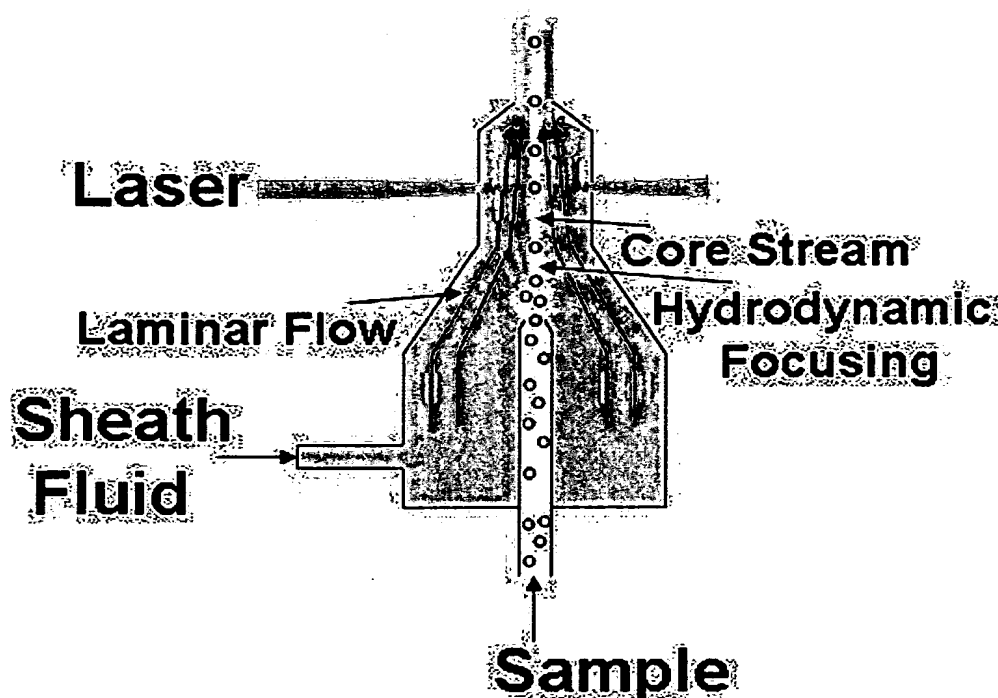
History – Flow cytometry of course simply means the measurement of cells while they are flowing through the detector system. Modern flow cytometry began in the late 1940s and early 1950s with Wallace Coulter's invention of the Coulter counter which measured the volume of cells by displacement of an electrolyte and subsequent increase in electrical impedance. Later principles and devices invented principally by Mack Fulwyler, Louis Kamentsky, Wolfgang Göhde, and Len Herzenberg's group at Stanford added new detection capabilities – measurement of size and granularity by light scatter and measurement of fluorescence. These devices all used light as the detection system. Len Herzenberg coined the term Fluorescence Activated Cell Sorting – FACS. The term FACS was used and trademarked by one of the manufacturers (B-D) so this class of instrument is now commonly referred to as flow cytometers. Concomitant developments that aided and expanded the utility of flow cytometers were the development of a vast array of fluorescent probes and especially the development of monoclonal antibodies pioneered by Cesar Milstein.

What can flow cytometry measure? – Flow cytometers can measure a diverse set of materials but it is required that the material to be analyzed be particulate. However that does not exclude the ability of a flow cytometer to measure soluble molecules. Virtually any component or function of cells can be measured as long as a fluorescent probe can be made that detects this. Many different types of cells can be analyzed - we have used bacteria, yeast, mammalian cells, and plant cells. Cellular subcomponents can be measured e.g chromosomes. In fact the human genome project started with the sorting of each of the chromosomes to simplify the analysis. Cell functions (e.g intracellular pH i.e. $[H^+]$, $[Na+]$, $[Zn+]$, phosphorylation status, membrane potential, DNA content) may be studied using flow cytometers. The development of a host of fluorescent reporter proteins (e.g green fluorescent protein – GFP) allows for easy interrogation of gene expression. To measure soluble molecules the molecules must first be trapped onto a particulate surface and then exposed by binding of fluorescent probes (e.g monoclonal antibodies). Indeed multiplexed assays can be developed that permit the simultaneous measurement of multiple analytes in the same sample.

How does a flow cytometer work (in brief!) – In order for a flow cytometer to work 4 areas of physics/technologies need to interplay. The first component is the fluidics system of the instrument. Because this is the mechanical component of the instrument most instrument problems are in the fluidics system. The heart of the fluidics system on all flow cytometers is the "nozzle". This is the component where cells are injected into the sheath fluid stream, are hydrodynamically focused, and in cuvette-nozzle designs where the cells are illuminated by the laser beams. Requirements for steering and focusing the laser beams and for collecting and detecting the fluorescence and scatter emissions require sophisticated optics. The collected light energy must be converted to electrical energy and this in turn converted to digital information. This is the function of the electronics of the cytometer. Finally in order for the operator/investigator to interpret what happened within the cytometer the data must be collected by a computer and interpreted by software into appropriate figures (histograms).
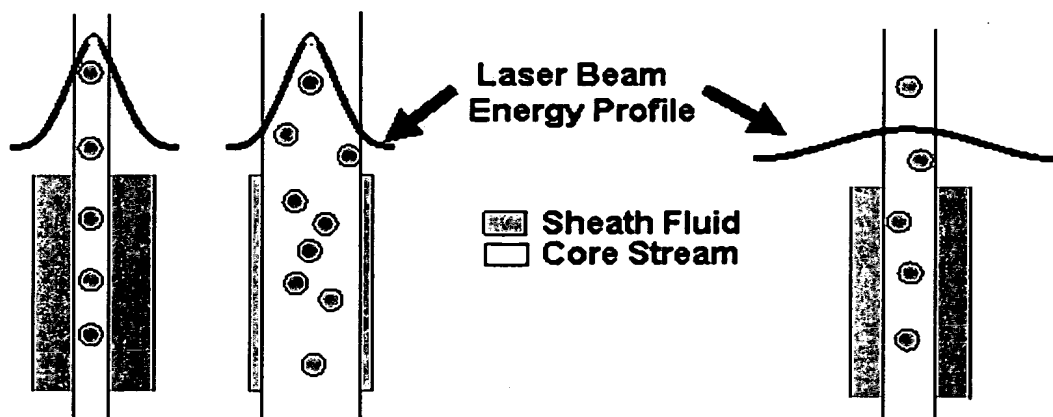
Attachment A

Fluidics - The fluidics system performs a number of critical functions. The first is to position the cells within the detector laser beam precisely and reproducibly. This is accomplished by using hydrodynamic focusing. The internal shape of the nozzle provides this effect in combination with an accelerating focusing fluid - the sheath fluid (normally simple PBS). The sample particles (cells) in single cell suspension (ideal) are injected into the sheath fluid stream. The figure to the left shows a representation of the major components of a cuvette nozzle design. The sample stream exits the sample injection needle and then via the effect of the hydrodynamic focusing is drawn out into a very small stream called the core stream (or sample stream). The diameter of the core stream is critical for both the accurate positioning of the cells in the laser(s) and for identifying when more than one cell is in the laser (doublets, triplets, etc.). The goal is to have the diameter of the core stream near to the diameter of the particles being analyzed. The diameter of the core stream varies in direct proportion to the pressure applied to the sample tube - less pressure = smaller diameter -- higher pressure = larger diameter. The quality of the data produced will always be better the smaller the core stream diameter is. However, the sample tube pressure also affects the rate at which cells are analyzed. Many users focus only on the event rate forgetting what increasing that by increasing sample pressure will do to the core stream diameter and thus to the quality of the data. While this may be acceptable for many cells up to a point, to obtain higher event rates while maintaining a tight core stream it is better to concentrate the sample and run at the lower sample pressure, if possible. In terms of correct positioning of the cells within the laser, the desire is to have the cells all go through the energy profile of the laser in the same place and, thus, be illuminated by the same number of photons. The energy profile across any diameter of the laser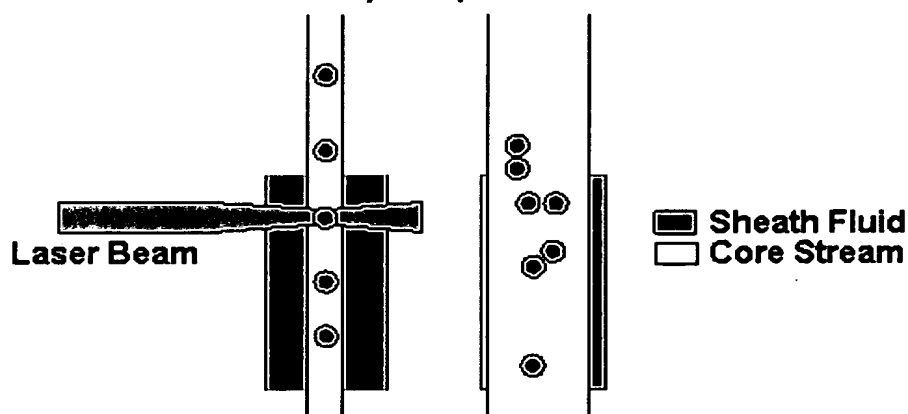 beam is Gaussian as shown. Of course, for many lower power lasers it is desirable that this transit point be at the peak of the laser energy distribution (as shown to the right). When the core stream is much wider than the cell diameter, cells, which distribute at random in the core stream, will pass through differing laser beam energy levels. This means that cells with the same amount of bound fluorochromes will be measured as having

slightly different levels resulting in a measurement error. The problem with precise laser beam localization is maximal when the cross-sectional area of the laser beam is spherical. Most flow cytometers now use lenses to reshape the laser beam to an elliptical cross-section (right most drawing figure above). This flattens and broadens the laser energy profile of the laser beam so that transit across the distribution reduces the positional laser energy that cells off-center experience and, thus, the problem is minimized. It still exits, however, and for applications (e.g. DNA content) where the CVs are critical still requires close attention to the core stream diameter. Flattening the energy profile does, however, have the adverse side effect of reducing the peak photon energy the cells experience and this loss may affect the resolution of the instrument unless the overall energy of the laser can be increased to offset this.

The second major function of the fluidics, that it accomplishes in part, is to deliver single cells to the interrogation laser. Assuming the cells exist as distinct individual cells, the hydrodynamic focusing, particularly when the sample pressure is such to have an appropriate core stream diameter, will put the cells in single file orientation and separate them sufficiently (on average) to have a single cell in the detection laser beam. However, even when cells are fully indepen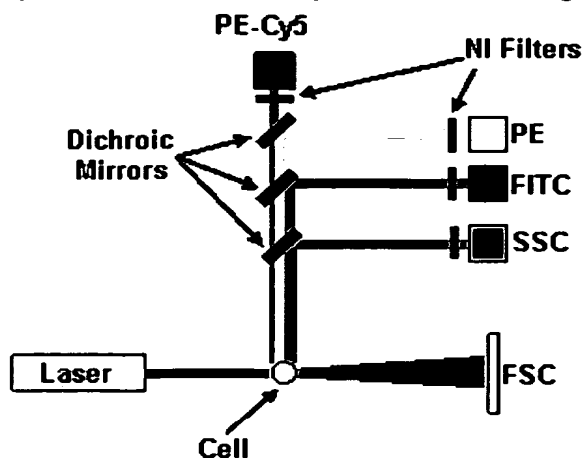dent of each other there is a statistical probability (described by the Poisson statistic) of more than a single cell being in the detector. Identifying with certainty that an event is a single cell is one of the major problems in using flow cytometry especially when analyzing rare events. Other methods are needed to confirm that such events are single cells (e.g. sorting to purify these events). As the sample pressure is increased and the core stream widens the frequency of doublet events will increase. This is shown in the figure to the left. As the core stream widens, cells may now be beside each other from the viewpoint of the laser.

Laser Beam

■ **Sheath Fluid**
□ **Core Stream**

We have at our disposal other methods to help identify when more than one cell is in the detector. In older flow cytometers (e.g. FACSCalibur, FACScan, and MoFlo) coincidence detection circuitry was employed to attempt to remove these doublet events. When an event triggered the system a time window was initiated and the circuitry looked to see if another event occurred with that window. A second event occurring in the window, while it could be detected, its data would not be resolvable from the first event and in the vast majority of analyses the data from both cells was rejected. Of course, if the cells became close enough together to not even be resolvable within the window time frame, the circuitry failed to detect the event as two cells. In the newer instruments (e.g CyAn, LSRII, MoFlo XDP, and Reflection) each event independently creates its own analysis window. This results in a much lower loss of data. However, events that are doublets are still not resolved as the doublet still creates only a single pulse and, thus, a single window. Pulse processing analysis allows us to identify many events as doublets and, thus, increase our confidence that events are not doublets - however, there is still a statistical probability that any given event that passes all these tests may not be a single cell. Pulse processing analysis permits use of the fact that for each pulse we may determine the height of the pulse (above threshold), the width of the pulse, and the area under the pulse. These properties have the same relationship for any single cell event regardless of the overall magnitude of the pulse but the relationships will be (may be) different for events that are composed two or more cells. For pulse processing to work best we must present the cells to the laser in the context of a properly sized core stream. When we do so doublets will have their long axis perpendicular to the laser and the event width will be maximized.

Optics - Since flow cytometers use light to make measurements it is no surprise that optical technologies are critical. Optical elements are required to both direct and shape the excitation laser beams but also to collect the light emitted from fluorescent probes. In order to measure and resolve data we must collect data in proper places and colors so that we know which parameter we are measuring. Flow cytometers routinely measure light scattered at two different angles (forward and side). Forward scatter is measured in the same direction (i.e. forward) as the laser beam is moving. Typically the forward scatter light is collected using a photodiode although a PMT (photomultiplier tube) can be used and is preferable for some applications. Forward scatter is typically and proportionally equated with size. However, forward scatter is even more so a function of refraction and. thus, directly inferring size must be done with caution. All other measurements in typical flow cytometers are made at some large angle (e.g. 90° relative to the primary laser beam) and use photomultiplier tubes (PMTs). The light is collected through sophisticated optical elements. In most instruments these are essentially microscope objective lens assemblies. However, the Reflection uses a novel light collection system that employs a parabolic reflector to collect the light. In some machines (e.g. LSRII and Reflection) the collected light is sent to the detectors via fiber optics. Side scatter signals measure the granularity or internal structure of the cell. Other PMTs are used for the various fluorochrome probes and the color of the light collected determines which probe is being measured. To isolate the color for each probe interference filters are used. Filters designed to work at normal incidence (NI) (i.e. 90° to the incoming light) are placed in front of each detector. A particular color of light is split off from the incoming mixture and directed to the detectors using interference filters designed to work at other angles (e.g. 45°) - called dichroic mirrors. A schematic of a 3-color system is shown.

Electronics - The electronics have several functions. The first is to convert the light information to analog electrical information, the second is to convert the analog (current/amp) electrical information to analog (voltage) information, then to convert the analog information to digital information that can be processed by the computer and software. The light enters the PMT and illuminates the photocathode. The absorption of light energy by the photocathode results in the release of photoelectrons from the photocathode. The photoelectrons are directed to the next element in the PMT, the first dynode, via an electrostatic field. Each photoelectron can release multiple electrons from the dynode since the photoelectron has more energy due to the acquisition of kinetic energy as it is repulsed from the photocathode and attracted to the more positively charged dynode. The number of electrons released from the photocathode per captured photon and subsequently from each dynode is a function of the electric potential (voltage) applied to the PMT by the flow operator. Thus, the number of electrons released at each step logarithmically propagates until all electrons are captured by the photoanode resulting in an electric current in the wire connected to the photoanode. This current, at a given PMT voltage, is proportional to the number of photons that entered the PMT. The next step is the conversion of the amperage to a voltage. This is the primary function (in addition to others such as baseline restoration) of the pre-amp. What follows after the pre-amp depends on what instrument one is using. Older designs (e.g. FACScan and FACSCalibur) used linear and logarithmic amplifiers to amplify and resolve signals. (The CyAn also uses log amps but in a slightly different way and in all other regards is like the all digital instruments). Log amps are used to increase the dynamic range so that signals of small and large magnitudes may be displayed on scale within the same histogram - a requirement for quantitative measurements. Log amps are never perfectly logarithmic which creates problems down stream when one uses pure mathematic approaches to deal with spectral

overlap between fluorochromes (compensation). The data from the amplifiers then goes to the ADCs (analog to digital converters) where the measured voltage is converted to a digital value. The value is based on the design of the ADC and its bit range (e.g. a 10-bit ADC will convert the lowest to highest voltage into numbers from 1 to 1024 (i.e. 2^{10}). Newer designs (MoFlo XDP, LSRII, and Reflection) do not have amplifiers but send data directly from the pre-amp to high resolution analog to digital converters to generate digital values of sufficient range to enable the use of log lookup tables to derive the logarithmic resolution needed. The electronics must also provide the means to align signals from different detectors, especially from detectors collecting light from additional spatially (and, thus, time) resolved lasers. In droplet sorters the electronics must also provide for the precise generation of droplets, the decision making of what cells are sorted, as well as other control elements that monitor other functions of the sorting process.

Computer/Software - The digital data values are received by the computer and the software translates this information into pictures (histograms - usually either single or dual parameter plots) that we can visually understand. We will not go into detail of the various software packages that are available. Please see a discussion of Summit by clicking here. Flow cytometry data files mostly conform to a standard - the FCS (flow cytometry standard) file structure (version FCS3.0 is the latest). The file structure permits not only the storage of the raw data from the detectors but also various other pieces of information about the sample and information about how it was collected (e.g. PMT voltages and compensation settings). The FCS file is also referred to as a "listmode file". In an FCS file all the raw data exists as separate pieces of information for every detector for each cell. The file structure allows users to later mix and match how they wish to combine various pieces of information to provide for a logical analysis of the information. One of the more powerful properties of flow software is the ability to generate regions of interest within one histogram and then to gate (restrict) a histogram displaying data for other parameters to only display the subset of information from the region of the first histogram. When analyzing two or more colors of fluorescence the emission from one fluorochrome may get into the detection channel of another fluorochrome. This must be dealt with by a process known as compensation (for a more complete discussion see Compensation in "Application Protocols" and appropriate discussions in "Instrument Protocols"). Algorithms now exist to help you with the proper adjustment of compensation.

Sorting - Sorting is the process where the flow cytometer (not all flow cytometers are sorters) physically separates cells and places them into test tubes. This can be done at high purity and rates, and keep the cells viable and sterile. All commercial sorters use the principles of electrostatic, droplet sorting. The first part of sorting is, of course, analysis and uses the basic principles described above. Cells of interest are marked in the flow cytometer and this information is used to make the sort decisions. In order to sort, the fluid stream containing the cells must be precisely (and reproducibly over a substantial time frame) broken into droplets - the cells will partition into the droplets. To do this an acoustical energy is supplied to the fluid within the nozzle and this energy travels down the fluid stream and causes the stream to divide into droplets. The sorter's computer can figure out which droplets will contain the cell of interest. When that droplet is the last attached droplet to the fluid stream an electric charge is placed on the stream and maintained until the droplet separates from the stream at which time the charge is reset to zero. Having detached from the stream and, thus, no longer connected to ground, the droplet retains the charge applied to it. The droplet then passes (falls) through a high energy electric field and the droplets are deflected by controlled amounts to fall into properly placed receptacles. The charge applied to the
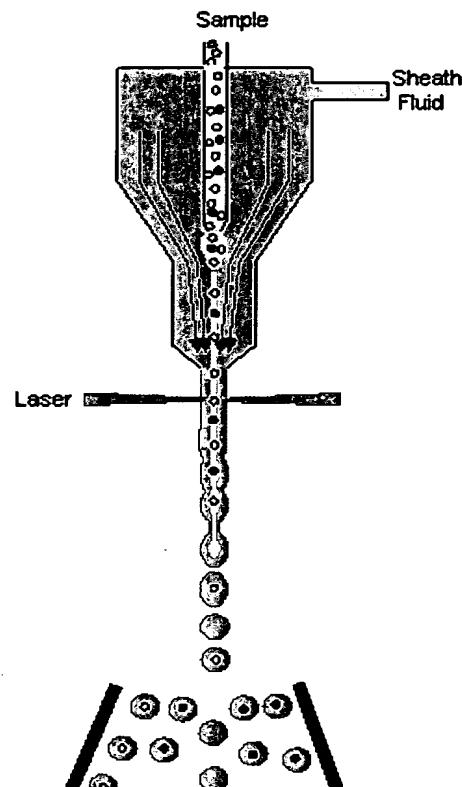
stream and to the droplets may be either positive or negative and, in addition, each may have two amplitudes. Thus, we can sort up to 4 streams and, thus, 4 populations simultaneously. The sorter may also be configured to deposit cells (as few as one per well) into various sized multi-well plates (up to 384 well configurations).

2

Molecular Cloning

SECOND EDITION

Conditions for Hybridization of Oligonucleotide Probes

When using oligonucleotides as probes, the aim is to find conditions that are stringent enough to guarantee specificity and sufficiently flexible to allow formation of stable hybrids at an acceptable rate. For DNA molecules more than 200 nucleotides in length, hybridization is usually carried out at 15–25°C below the calculated melting temperature (T_m) of a perfect hybrid. However, as the length of the probe is decreased, the T_m is lowered to the point where it is often impractical to carry out hybridization at $T_m - 25$°C. Typically, therefore, hybridization with synthetic oligonucleotides is carried out under conditions that are only 5–10°C below the T_m. Although such stringent conditions reduce the number of mismatched clones that are detected with short oligonucleotide probes, they have the less desirable consequence of reducing the rate at which perfect hybrids form.

Hybrids formed between DNA molecules more than 200 nucleotides in length are completely stable for all practical purposes. The chances that such a long stretch of double helix will unwind at temperatures 15–25°C below the T_m are extremely small. However, hybrids (even perfect hybrids) formed between short oligonucleotides and their target sequences at 5–10°C below the T_m are far easier to unwind, and hybridization reactions of this type can be regarded as reversible. This has important practical consequences. Whereas hybrids formed between longer DNA molecules are essentially stable under the conditions used for posthybridization washing, hybrids (even perfect hybrids) involving short oligonucleotides are not. Posthybridization washing of such hybrids must therefore be carried out rapidly so that the probe does not dissociate from its target sequence. For this reason, hybridizations with short oligonucleotides should be carried out under stringent conditions (5–10°C below the T_m) using high concentrations (0.1–1.0 pmole/ml) of probe. When only one or a small number of oligonucleotides (<8) are used as probes, the annealing reaction rapidly reaches equilibrium, and hybridization should therefore be terminated after 3 or 4 hours. More complex mixtures, in which the concentration of each oligonucleotide is comparatively low, require hybridization to be carried out for proportionately longer periods. For example, mixtures of 32 or more oligonucleotides should be hybridized for 1–2 days. Posthybridization washing should be carried out for brief periods of time, initially under conditions of low stringency and then under conditions of stringency equal to those used for hybridization.

CALCULATING MELTING TEMPERATURES FOR PERFECTLY MATCHED HYBRIDS BETWEEN OLIGONUCLEOTIDES AND THEIR TARGET SEQUENCES

When using single oligonucleotides that match the target sequence perfectly, hybridization conditions can easily be derived from the calculated T_m of the hybrid. For oligonucleotides shorter than 18 nucleotides, the T_m of the hybrid can be estimated by multiplying the number of A + T residues in the hybrid by 2°C and the number of G + C residues by 4°C and adding the two numbers (Itakura et al. 1984). However, this method overestimates the T_m of hybrids involving longer oligonucleotides.

A different approach has been taken by E. Fritsch (unpubl.), who found that the equation originally used to calculate the relationship between G + C content, ionic strength of the hybridization solution, and the T_m of long DNA molecules (Bolton and McCarthy 1962):

$$T_m = 81.5 + 16.6(\log_{10}[Na^+]) + 0.41(\text{fraction G + C}) - (600/N),$$

where N = chain length, predicts reasonably well the T_m for oligonucleotides as long as 60–70 nucleotides and as short as 14 nucleotides.

This formula only works for Na^+ concentrations of 1 M or less.

ESTIMATING THE EFFECTS OF MISMATCHES

Perhaps surprisingly, the classic formula (Bonner et al. 1973) to calculate the effect of mismatches on the stability of long DNA hybrids holds reasonably well for hybrids involving short oligonucleotides: For every 1% of mismatching of bases in a double-stranded DNA, there is a reduction of T_m by 1–1.5°C. However, the precise effect of mismatches depends on the G + C content of the oligonucleotide and, even more critically, on the distribution of mismatched bases in the double-stranded DNA. Mismatches in the middle of the oligonucleotide are far more deleterious than mismatches at the ends. Therefore, the method of estimation given above should only be used as a rough guide until a systematic study of all types of mismatches in a variety of contexts leads to more precise methods of estimation. If appropriate target DNA has been cloned, the effect of mismatches on T_m can be determined empirically (see pages 11.55–11.57).

It is easy to calculate accurately the T_m of a perfectly matched hybrid formed between a single oligonucleotide and its target sequence. However, when using pools of oligonucleotides whose members have greatly different contents of G + C, it is impossible to estimate a consensus T_m. Because it is not possible to know which member of the pool will match the target sequence perfectly, conditions must be used that allow the oligonucleotide with the lowest content of G + C to hybridize efficiently. Usually, conditions are chosen to be 2°C below the calculated T_m of the most A/T-rich member of the pool (Suggs et al. 1981b). However, the use of such "lowest common denominator" conditions can lead to a number of false positives, because mismatched hybrids formed by oligonucleotides of higher G + C content may be more stable than a perfectly matched hybrid formed by the correct oligonucleotide. In most cases, this problem is not serious, since the number of positive clones obtained by screening cDNA libraries with pools of oligonucleotides is usually quite manageable. It is therefore possible to easily distinguish false positives from true positives by another test (e.g., DNA sequencing or hybridization with a second pool of oligonucleotides corresponding to another segment of amino acid sequence).

In those cases when the number of positives is unacceptably high, it may be worthwhile to consider using hybridization solvents that contain the quaternary alkylammonium salts tetraethylammonium chloride (TEACl) or tetramethylammonium chloride (TMACl) instead of sodium chloride (Melchior and von Hippel 1973; Jacobs et al. 1985, 1988; Wood et al. 1985; Gitschier et al. 1986; Wozney 1989). In these solvents, the T_m of a hybrid is independent of its base composition and dependent primarily on its length. Thus, by choosing a temperature for hybridization appropriate for the lengths of the oligonucleotides in a pool, the effects of potential mismatches can be minimized.

It is important to obtain an accurate estimate of the T_m in TMACl or TEACl before using pools of oligonucleotides to screen cDNA or genomic DNA libraries. Jacobs et al. (1988) measured the T_i (the irreversible melting temperature of the hybrid formed between the probe and its target sequence) as a function of chain length for a number of oligonucleotides of differing G + C content in solvents containing either sodium or tetramethylammonium ions. Hybrids involving oligonucleotides 16 and 19 nucleotides in length melt over a smaller range of temperature in solvents containing TMACl than in solvents containing sodium salts (3°C for TMACl vs. 17°C for SSC when hybridizing 16-mers; 5°C for TMACl vs. 20°C for SSC when hybridizing 19-mers). For 14-mers, the effect is much less dramatic (7°C for TMACl vs. 9°C for SSC). Similar, but less extensive, data are available for solvents containing TEACl (Jacobs et al. 1988).

The optimal temperature for hybridization is usually chosen to be 5°C below the T_i for the given chain length. The recommended hybridization temperature for 17-mers in 3 M TMACl is 48–50°C; for 19-mers, it is 55–57°C; and for 20-mers, it is 58–66°C. Three points are worth emphasizing. First, the T_is of hybrids are uniformly 15–20°C higher in solvents containing TMACl than in solvents containing TEACl. The higher T_i in solvents containing TMACl allows hybridization to be performed at temperatures that

suppress nonspecific adsorption of the probe to solid supports (such as nylon membranes), resulting in lower nonspecific backgrounds. Second, hybridization solvents containing TMACl do not have significant advantages over those containing sodium ions until the length of the oligonucleotide exceeds 16 nucleotides. Finally, the data have been extensively examined for 16-mers, 19-mers, and, in previous studies, for much longer DNA molecules (Melchior and von Hippel 1973). It is currently an untested assumption that the same beneficial effect will be seen for DNA molecules of all intermediate lengths.

Preparation and Use of Solvents Containing Quaternary Alkylammonium Salts

1. Prepare a 6 M solution of tetramethylammonium chloride (TMACl) or a 3 M solution of tetraethylammonium chloride (TEACl) in H_2O. (TMACl and TEACl are available from Aldrich.)

2. Add activated charcoal to a final concentration of approximately 10% and stir for 20–30 minutes.

3. Allow the charcoal to settle, and then filter the solution of TMACl or TEACl through a Whatman No. 1 paper.

4. Filter the solution through a nitrocellulose filter (e.g., Nalge, 0.45-micron pore size). Store the filtered solution in dark bottles at room temperature.

5. Measure the refractive index of the solution, and calculate the precise concentration of the solution from the equation:

$$C = (n - 1.331)/0.018$$

where C = molar concentration of quaternary alkylammonium salt and n = refractive index.

6. Prehybridize nitrocellulose filters or nylon membranes for 2–6 hours in oligonucleotide prehybridization solution.

Oligonucleotide prehybridization solution

6× SSC (or 6× SSPE)
0.01 M sodium phosphate (pH 6.8)
1 mM EDTA (pH 8.0)
0.5% SDS
100 μg/ml denatured, fragmented salmon sperm DNA (see Appendix B)
0.1% nonfat dried milk

7. Prepare the quaternary alkylammonium solution to be used for hybridization:

Quaternary alkylammonium hybridization solution

3.0 M TMACl or 2.4 M TEACl
0.01 M sodium phosphate (pH 6.8)
1 mM EDTA (pH 7.6)
0.5% SDS
100 μg/ml denatured, fragmented salmon sperm DNA
0.1% nonfat dried milk

Notes

i. Nitrocellulose filters are not stable when hybridization is carried out for extended periods of time in solvents containing TMACl or TEACl. Nylon membranes are much better suited for this purpose.

ii. Posthybridization washing is usually carried out initially with solutions containing sodium salts (e.g., $6 \times$ SSC) rather than quaternary alkylammonium salts. If additional stringent washes are required, rinse the filters first with quaternary alkylammonium hybridization solution (without DNA or nonfat dried milk) at room temperature and then briefly (5–10 minutes) with the same solution at $T_i - 5°C$.

HYBRIDIZATION OF GUESSMERS

Perhaps the most critical step in the use of guessmers is the choice of conditions for hybridization. The temperature should be high enough to suppress hybridization of the probe to incorrect sequences but must not be so high as to prevent hybridization to the correct sequence, even though it may be mismatched. Before using an oligonucleotide to screen a library, it is therefore advisable to perform a series of trial experiments in which a series of northern or genomic Southern hybridizations are carried out under different degrees of stringency (Anderson and Kingston 1983; Wood et al. 1984). A set of theoretical curves relating the temperature of the washing solution to the length and homology of the probe is given in Lathe (1985). Using these curves as a guide, determine the optimal conditions for detection of sequences complementary to the probe by hybridizing the oligonucleotide to a series of nitrocellulose filters or nylon membranes at different temperatures. The filters are washed extensively in 6× SSC at room temperature and then briefly (5–10 minutes in 6 × SSC) at the temperature used for hybridization. This method, in which both hybridization and washing are carried out under the same conditions of temperature and ionic strength, appears to be more discriminating than the more commonly used procedure of hybridizing under conditions of lower stringency and washing under conditions of higher stringency.

If trial experiments are not possible, attempt to estimate the melting temperature (T_m) as follows:

1. Calculate the minimum G + C content of the oligonucleotide assuming that A or T is present at all positions of ambiguity.

2. Using the following formula, calculate the T_m of a double-stranded DNA with the calculated G + C content:

   $$T_m = 81.5 + 16.6(\log_{10}[\text{Na}^+]) + 0.41(\text{fraction G} + \text{C}) - (600/N)$$

   where N = chain length.

   This formula only works for Na^+ concentrations of 1 M or less.

3. Calculate the maximum amount of possible mismatch assuming that all choices of degenerate codons are incorrect. Subtract 1°C from the calculated T_m for each 1% of mismatch. The resulting number should be the T_m of a maximally mismatched hybrid formed between the probe and its target DNA sequence.

In the absence of information from trial experiments, hybridization and washing should be carried out at 5–10°C below the estimated T_m. Almost certainly, the actual T_m will be higher than that predicted by this worst-case calculation. If the bases used at positions of ambiguity were chosen at random, one out of four should be correct, and approximately half of these would be expected to be G or C. The observed T_m should therefore be significantly higher than that estimated. However, to minimize the risk of missing the clone of interest, it is best to hybridize and wash at several degrees below the T_m estimated as described above. If, under these conditions, the probe hybridizes indiscriminately, repeat the hybridization at a higher temperature or wash under conditions of higher stringency.

Before proceeding to screen an entire cDNA or genomic DNA library, it is advisable to carry out a series of pilot experiments in which the probe is hybridized under different conditions to small aliquots (perhaps 5000–10,000 clones) of the library that is to be screened. The results of these experiments should allow you to choose conditions for large-scale screening that are just stringent enough to eliminate nondiscriminate hybridization of the probe to the vast majority of clones in the library.

Hybridization of guessmers in solvents that contain quaternary alkylammonium salts has not been investigated.

HYBRIDIZATION OF OLIGONUCLEOTIDES THAT CONTAIN A NEUTRAL BASE AT POSITIONS OF DEGENERACY

Although the conditions for hybridization of probes that contain the neutral base inosine have not been extensively explored, it is possible to make a conservative estimate of the melting temperature (T_m) as follows:

1. Subtract the number of inosine residues from the total number of nucleotides in the probe to give a value S.

2. Calculate the $G + C$ content of S.

3. Estimate the T_m of a perfect hybrid involving S using the equation on page 11.52.

4. Use conditions for hybridization that are 15–20°C below the estimated T_m.

The T_m of hybrids involving oligonucleotides that contain neutral bases can also be estimated empirically as described on pages 11.55–11.57. Hybridization of such oligonucleotides in solvents containing quaternary alkylammonium salts has not been investigated.

EMPIRICAL DETERMINATION OF MELTING TEMPERATURE

The melting temperature (T_m) of an oligonucleotide hybridized to a target sequence can be determined by the procedure described below. The protocol actually measures the temperature at which dissociation of the double-stranded DNA becomes irreversible (T_i) in nonequilibrium conditions that do not favor rehybridization of the released probe to the target. The optimal temperature for hybridization is then determined on the basis of this value. The procedure requires a cloned target sequence that is complementary (perfectly or imperfectly, depending on the experiment) to the oligonucleotide probe. In most cases, a target sequence is not available from "natural" sources and must be synthesized chemically. The best synthetic target sequences consist of two oligonucleotides that are partially complementary. After annealing, these oligonucleotides form a double-stranded region that contains the target sequence. The sequences of the protruding ends are designed to allow the target DNA to be cloned easily in bacteriophage M13 vectors. Single-stranded DNA of the appropriate orientation prepared from the resulting clones (see Chapter 4) can be used in hybridization experiments as described below. It can also be used as a template for dideoxy-mediated chain-termination sequencing (see Chapter 13) if it is necessary to check that the sequence of the target DNA is correct.

1. Label 1–10 pmoles of the oligonucleotide to be used as a probe by phosphorylation (see pages 11.31–11.32), and remove excess unincorporated [γ-^{32}P]ATP by one of the methods described on pages 11.33–11.39.

2. Using a paper punch, prepare four small circles (diameter 3–4 mm) of a solid support (nitrocellulose filter or nylon membrane) used for hybridization. Arrange the small circles on a piece of Parafilm. Mark two of the filters with a soft-lead pencil.

3. Apply approximately 100 ng of target single-stranded DNA in a volume of 1–3 μl of 2× SSC to each of the marked filters. Apply an equal amount of vector DNA to the unmarked filters. After the fluid has dried, use blunt-ended forceps (e.g., Millipore forceps) to remove the two sets of filters from the Parafilm, and place them between sheets of Whatman 3MM paper. Fix the DNAs to the filters by baking for 1–2 hours at 80°C in a vacuum oven.

   If the target DNA has been cloned into a plasmid, linearize the vector by digestion with a restriction enzyme that does not cleave within the target sequences. Purify the resulting double-stranded DNA by extraction with phenol:chloroform and precipitation with ethanol. Dissolve the DNA in 2× SSC at a concentration of 500 ng/μl. Apply the solution of DNA to the filters prepared as described above, and then, using blunt-ended forceps, transfer the filters to a sheet of 3MM paper saturated with denaturing solution (1.5 M NaCl, 0.5 N NaOH) for 5–10 minutes. Move the filters to a fresh sheet of 3MM paper saturated with neutralizing solution (0.5 M Tris·Cl [pH 7.4], 1.5 M NaCl) for 10 minutes. Transfer the filters to a dry sheet of 3MM paper, and leave them at room temperature until all of the fluid has evaporated. Bake the filters as described above.

   Overbaking can cause the filters to become brittle. In addition, filters that have not been completely neutralized turn yellow or brown during baking and chip very easily. The background of nonspecific hybridization also increases dramatically.

4. Using blunt-ended forceps, transfer all of the filters to a polyethylene tube that contains 2 ml of oligonucleotide prehybridization solution. Seal the tube and incubate, with occasional shaking, at a temperature estimated to be $T_m - 25°C$ for the solvent being used (see Note i). After 2 hours, add radiolabeled oligonucleotide to the prehybridization solution. The final concentration of oligonucleotide should be approximately 1 pmole/ml. Continue incubation at $T_m - 25°C$ for a further 2–4 hours, with occasional shaking.

Oligonucleotide prehybridization solution

6× SSC (or 6× SSPE)
0.01 M sodium phosphate (pH 6.8)
1 mM EDTA (pH 8.0)
0.5% SDS
100 μg/ml denatured, fragmented salmon sperm DNA (see Appendix B)
0.1% nonfat dried milk

5. Remove the filters from the hybridization solution, and immediately immerse them in 2× SSC at room temperature. Agitate the fluid continuously. Replace the fluid every 5 minutes until the amount of radioactivity on the filters remains constant (as measured with a hand-held minimonitor).

6. Adjust the temperature of a circulating water bath to $T_m - 25°C$. Dispense 5 ml of 2× SSC into each of 20 glass test tubes (17 mm × 100 mm). Monitor the temperature of the fluid in one of the tubes with a thermometer. Incubate the tubes in the water bath until the temperature of the 2× SSC is $T_m - 25°C$. The 2× SSC in each of these tubes will be used separately for each temperature increase (see steps 7–10).

7. Transfer the filters individually to four empty glass tubes, separating the filters containing the vector and target DNAs, and add 1 ml of 2× SSC (from one of the tubes prepared in step 6 and prewarmed to $T_m - 25°C$). Place the tubes in the water bath for 5 minutes.

8. Remove the tubes from the bath, transfer the liquid to scintillation vials, and wash the tubes and filters with 1 ml of 2× SSC at room temperature. Add the wash solutions to the appropriate scintillation vials.

9. Increase the temperature of the water bath by 3°C, and wait for the temperature of the 2× SSC in the tubes prepared in step 6 to equilibrate.

10. Add 1 ml of 2× SSC at the higher temperature to each of the four tubes containing the filters. Place the tubes in the water bath for 5 minutes.

11. Repeat steps 8, 9, and 10 at successively higher temperatures until a temperature of $T_m + 30°C$ is achieved.

12. Place the filters in separate glass tubes (17 mm × 100 mm) containing 1 ml of 2 × SSC, and heat them to boiling for 5 minutes to remove any remaining radioactivity. Cool the solutions in ice, and transfer them to scintillation vials. Wash the filters and tubes used for boiling with 1 ml of 2 × SSC, and add the washing solutions to the appropriate scintillation vials.

13. Use a scintillation counter to measure the radioactivity (by Cerenkov counting, see Appendix E) in all of the vials. Calculate the proportion of the total radioactivity that has eluted at each temperature (i.e., the sum of radioactivity eluted at all temperatures between $T_m - 25°C$ and the temperature at which a given sample was taken divided by the total radioactivity eluted from the filters at all temperatures up to and including 100°C).

   If the experiment has worked well, very little radioactivity should be associated with the filters containing vector DNA alone. Furthermore, this radioactivity should be completely released from the filters at temperatures much lower than the estimated T_m. On the other hand, considerable radioactivity should be associated with the filters containing the target DNA; the elution of this radioactivity should show a sharp temperature dependence. Very little radioactivity should be released from the filters until a critical temperature is reached, and then approximately 90% of the radioactivity should be released during the succeeding 6-9°C rise in temperature. The temperature at which 50% of the radioactivity has eluted from the filters containing the target sequences is defined as the T_i of the hybrid between the probe and its target sequence.

Notes

i. Although the above protocol calls for the use of sodium salts in the solvent used for hybridization, other solutes such as tetramethylammonium chloride or tetraethylammonium chloride can be substituted if desired to determine the T_i in these solvents.

ii. This method can easily be adapted to study the behavior of hybrids formed between probes and target sequences that do not match each other perfectly (Jacobs et al. 1988).

iii. Before synthesizing the probe, check for potential homology and/or complementarity between its sequence and the sequence of the vector used to propagate the target. Most of the commercially available programs to analyze DNA can be used to search commonly used vectors for sequences that match the sequence of the probe closely enough to cause problems during hybridization.

References

Abraham, J.A., A. Mergia, J.L. Whang, A. Tumolo, J. Friedman, K.A. Hjerrild, D. Gospodarowicz, and J.C. Fiddes. 1986. Nucleotide sequence of a bovine clone encoding the bovine angiogenic protein, basic fibroblast growth factor. *Science* **233:** 545.

Anderson, S. and I.B. Kingston. 1983. Isolation of a genomic clone for bovine pancreatic trypsin inhibitor by using a unique-sequence synthetic DNA probe. *Proc. Natl. Acad. Sci.* **80:** 6838.

Benedum, U.M., P.A. Baeuerle, D.S. Konecki, R. Frank, J. Powell, J. Mallet, and W.B. Huttner. 1986. The primary structure of bovine chromogranin A: A representative of a class of acidic secretory proteins common to a variety of peptidergic cells. *EMBO J.* **5:** 1495.

Bennetzen, J.L. and B.D. Hall. 1982. Codon selection in yeast. *J. Biol. Chem.* **257:** 3026.

Betsholtz, C., A. Johnsson, C.-H. Heldin, B. Westermark, P. Lind, M.S. Urdea, R. Eddy, T.B. Shows, K. Philpott, A.L. Mellor, T.J. Knott, and J. Scott. 1986. cDNA sequence and chromosomal localization of human platelet-derived growth factor A-chain and its expression in tumour cell lines. *Nature* **320:** 695.

Bird, A.P. 1980. DNA methylation and the frequency of CpG in animal DNA. *Nucleic Acids Res.* **8:** 1499.

Bolton, E.T. and B.J. McCarthy. 1962. A general method for the isolation of RNA complementary to DNA. *Proc. Natl. Acad. Sci.* **48:** 1390.

Bonner, T.I., D.J. Brenner, B.R. Neufeld, and R.J. Britten. 1973. Reduction in the rate of DNA reassociation by sequence divergence. *J. Mol. Biol.* **81:** 123.

Bray, P., A. Carter, C. Simons, V. Guo, C. Puckett, J. Kamholz, A. Spiegel, and M. Nirenberg. 1986. Human cDNA clones for four species of $G_{\alpha s}$ signal transduction protein. *Proc. Natl. Acad. Sci.* **83:** 8893.

Celeste, A.J., V. Rosen, J.L. Buecker, R. Kriz, E.A. Wang, and J.M. Wozney. 1986. Isolation of the human gene for bone gla protein utilizing mouse and rat cDNA clones. *EMBO J.* **5:** 1885.

Davis, T.N. and J. Thorner. 1987. Isolation of the yeast calmodulin gene using synthetic oligonucleotide probes. *Methods Enzymol.* **139:** 248.

Derynck, R., A.B. Roberts, M.E. Winkler, E.Y. Chen, and D.V. Goeddel. 1984. Human transforming growth factor-α: Precursor structure and expression in *E. coli. Cell* **38:** 287.

Derynck, R., J.A. Jarrett, E.Y. Chen, D.H. Eaton, J.R. Bell, R.K. Assoian, A.B. Roberts, M.B. Sporn, and D.V. Goeddel. 1985. Human transforming growth factor-β complementary DNA sequence and expression in normal and transformed cells. *Nature* **316:** 701.

Docherty, A.J.P., A. Lyons, B.J. Smith, E.M. Wright, P.E. Stephens, T.J.R. Harris, G. Murphy, and J.R. Reynolds. 1985. Sequence of human tissue inhibitor of metalloproteinases and its identity to erythroid-potentiating activity. *Nature* **318:** 66.

Geck, P. and I. Nász. 1983. Concentrated, digestible DNA after hydroxylapatite chromatography with cetylpyridinium bromide precipitation. *Anal. Biochem.* **135:** 264.

Gitschier, J., W.I. Wood, M.A. Shuman, and R.M. Lawn. 1986. Identification of a missense mutation in the factor VIII gene of a mild hemophiliac. *Science* **232:** 1415.

Goeddel, D.V., E. Yelverton, A. Ullrich, H.L. Heyneker, G. Miozzari, W. Holmes, P.H. Seeburg, T. Dull, L. May, N. Stebbing, R. Crea, S. Maeda, R. McCandliss, A. Sloma, J.M. Tabor, M. Gross, P.C. Familletti, and S. Pestka. 1980. Human leukocyte interferon produced by *E. coli* is biologically active. *Nature* **287:** 411.

Grantham, R., C. Gautier, M. Gouy, M. Jacobzone, and R. Mercier. 1981. Codon catalog usage is a genome strategy modulated for gene expressivity. *Nucleic Acids Res.* (suppl.) **9:** 43.

Grantham, R., C. Gautier, M. Gouy, R.

Mercier, and A. Pavé. 1980. Codon catalog usage and the genome hypothesis. *Nucleic Acids Res.* (suppl.) **8:** 49.

Grundmann, U., E. Amann, G. Zettlmeissl, and H.A. Küpper. 1986. Characterization of cDNA coding for human factor XIIIa. *Proc. Natl. Acad. Sci.* **83:** 8024.

Hewick, R.M., M.W. Hunkapiller, L.E. Hood, and W.J. Dreyer. 1981. A gas-liquid solid phase peptide and protein sequenator. *J. Biol. Chem.* **256:** 7990.

Hoekema, A., R.A. Kastelein, M. Vasser, and H.A. de Boer. 1987. Codon replacement in the *PGK1* gene of *Saccharomyces cerevisiae:* Experimental approach to study the role of biased codon usage in gene expression. *Mol. Cell. Biol.* **7:** 2914.

Hunkapiller, M.W., E. Lujan, F. Ostrander, and L.E. Hood. 1983. Isolation of microgram quantities of proteins from polyacrylamide gels for amino acid sequence analysis. *Methods Enzymol.* **91:** 227.

Ikuta, S., K. Takagi, R.B. Wallace, and K. Itakura. 1987. Dissociation kinetics of 19 base paired oligonucleotide-DNA duplexes containing different single mismatched base pairs. *Nucleic Acids Res.* **15:** 797.

Itakura, K., J.J. Rossi, and R.B. Wallace. 1984. Synthesis and use of synthetic oligonucleotides. *Annu. Rev. Biochem.* **53:** 323.

Itakura, K., T. Hirose, R. Crea, A.D. Riggs, H.L. Heyneker, F. Bolivar, and H.W. Boyer. 1977. Expression in *Escherichia coli* of a chemically synthesized gene for the hormone somatostatin. *Science* **198:** 1056.

Jacobs, K.A., R. Rudersdorf, S.D. Neill, J.P. Dougherty, E.L. Brown, and E.F. Fritsch. 1988. The thermal stability of oligonucleotide duplexes is sequence independent in tetraalkylammonium salt solutions: Application to identifying recombinant DNA clones. *Nucleic Acids Res.* **16:** 4637.

Jacobs, K., C. Shoemaker, R. Rudersdorf, S.D. Neill, R.J. Kaufman, A. Mufson, J. Seehra, S.S. Jones, R. Hewick, E.F. Fritsch, M. Kawakita, T. Shimizu, and T. Miyake. 1985. Isolation and characterization of genomic and cDNA clones of human erythropoietin. *Nature* **313:** 806.

Jaye, M., H. de la Salle, F. Schamber, A. Balland, V. Kohli, A. Findeli, P. Tol-

stoshev, and J.-P. Lecocq. 1983. Isolation of a human anti-haemophilic factor IX cDNA clone using a unique 52-base synthetic oligonucleotide probe deduced from the amino acid sequence of bovine factor IX. *Nucleic Acids Res.* **11:** 2325.

Jaye, M., R. Howk, W. Burgess, G.A. Ricca, I.-M. Chiu, M.W. Ravera, S.J. O'Brien, W.S. Modi, T. Maciag, and W.N. Drohan. 1986. Human endothelial cell growth factor: Cloning, nucleotide sequence, and chromosome localization. *Science* **233:** 541.

Kent, S., L. Hood, R. Aebersold, D. Teplow, L. Smith, V. Farnsworth, P. Cartier, W. Hines, P. Hughes, and C. Dodd. 1987. Approaches to sub-picomole protein sequencing. *BioTechniques* **5:** 314.

Knopf, J.L., M.-H. Lee, L.A. Sultzman, R.W. Kriz, C.R. Loomis, R.M. Hewick, and R.M. Bell. 1986. Cloning and expression of multiple protein kinase C cDNAs. *Cell* **46:** 491.

Laird, C.D. 1971. Chromatid structure: Relationship between DNA content and nucleotide sequence diversity. *Chromosoma* **32:** 378.

Lathe, R. 1985. Synthetic oligonucleotide probes deduced from amino acid sequence data: Theoretical and practical considerations. *J. Mol. Biol.* **183:** 1.

Lauffer, L., P.D. Garcia, R.N. Harkins, L. Coussens, A. Ullrich, and P. Walter. 1985. Topology of signal recognition particle receptor in endoplasmic reticulum membrane. *Nature* **318:** 334.

Lewis, V.A., T. Koch, H. Plutner, and I. Mellman. 1986. A complementary DNA clone for a macrophage-lymphocyte Fc receptor. *Nature* **324:** 372.

Lin, F.-K., S. Suggs, C.-H. Lin, J.K. Browne, R. Smalling, J.C. Egrie, K.K. Chen, G.M. Fox, F. Martin, Z. Stabinsky, S.M. Badrawi, P.-H. Lai, and E. Goldwasser. 1985. Cloning and expression of the human erythropoietin gene. *Proc. Natl. Acad. Sci.* **82:** 7580.

Lo, K.-M., S.S. Jones, N.R. Hackett, and H.G. Khorana. 1984. Specific amino acid substitutions in bacterioopsin: Replacement of a restriction fragment in the structural gene by synthetic DNA fragments containing altered codons. *Proc. Natl. Acad. Sci.* **81:** 2285.

Martin, F.H., M.M. Castro, F. Aboul-ela, and I. Tinoco, Jr. 1985. Base pairing involving deoxyinosine: Implications

for probe design. *Nucleic Acids Res.* 13: 8927.

Mason, A.J., J.S. Hayflick, N. Ling, F. Esch, N. Ueno, S.-Y. Ying, R. Guillemin, H. Niall, and P.H. Seeburg. 1985. Complementary DNA sequences of ovarian follicular fluid inhibin show precursor structure and homology with transforming growth factor-β. *Nature* 318: 659.

Melchior, W.B. and P.H. von Hippel. 1973. Alteration of the relative stability of dA·dT and dG·dC base pairs in DNA. *Proc. Natl. Acad. Sci.* 70: 298.

Montgomery, D.L., B.D. Hall, S. Gillam, and M. Smith. 1978. Identification and isolation of the yeast cytochrome c gene. *Cell* 14: 673.

Nagata, S., M. Tsuchiya, S. Asano, Y. Kaziro, T. Yamazaki, O. Yamamoto, Y. Hirata, N. Kubota, M. Oheda, H. Nomura, and M. Ono. 1986. Molecular cloning and expression of cDNA for human granulocyte colony-stimulating factor. *Nature* 319: 415.

Narang, S.A. 1983. DNA synthesis. *Tetrahedron* 39: 3.

Narang, S.A., R. Brousseau, H.M. Hsiung, and J.J. Michniewicz. 1980. Chemical synthesis of deoxyoligonucleotides by the modified triester method. *Methods Enzymol.* 65: 610.

Newgard, C.B., K. Nakano, P.K. Hwang, and R.J. Fletterick. 1986. Sequence analysis of the cDNA encoding human liver glycogen phosphorylase reveals tissue-specific codon usage. *Proc. Natl. Acad. Sci.* 83: 8132.

Ohtsuka, E., S. Matsuki, M. Ikehara, Y. Takahashi, and K. Matsubara. 1985. An alternative approach to deoxyoligonucleotides as hybridization probes by insertion of deoxyinosine at ambiguous codon positions. *J. Biol. Chem.* 260: 2605.

Pennica, D., G.E. Nedwin, J.S. Hayflick, P.H. Seeburg, R. Derynck, M.A. Palladino, W.J. Kohr, B.B. Aggarwal, and D.V. Goeddel. 1984. Human tumour necrosis factor: Precursor structure, expression and homology to lymphotoxin. *Nature* 312: 724.

Rossi, J.J., R. Kierzek, T. Huang, P.A. Walker, and K. Itakura. 1982. An alternate method for synthesis of double-stranded DNA segments. *J. Biol. Chem.* 257: 9226.

Sanchez-Pescador, R. and M.S. Urdea. 1984. Use of unpurified synthetic de-

oxynucleotide primers for rapid dideoxynucleotide chain termination sequencing. *DNA* 3: 339.

Sharp, P.M., E. Cowe, D.G. Higgins, D.C. Shields, K.H. Wolfe, and F. Wright. 1988. Codon usage patterns in *Escherichia coli, Bacillus subtilis, Saccharomyces cerevisiae, Schizosaccharomyces pombe, Drosophila melanogaster* and *Homo sapiens;* a review of the considerable within-species diversity. *Nucleic Acids Res.* 16: 8207.

Sibatani, A. 1970. Precipitation and counting of minute quantities of labeled nucleic acids as cetyltrimethylammonium salt. *Anal. Biochem.* 33: 279.

Smith, M. 1983. Synthetic oligodeoxyribonucleotides as probes for nucleic acids and as primers in sequence determination. In *Methods of DNA and RNA sequencing* (ed. S.M. Weissman), p. 23. Praeger Publishers, New York.

Sood, A.K., D. Pereira, and S.M. Weissman. 1981. Isolation and partial nucleotide sequence of a cDNA clone for human histocompatibility antigen HLA-B by use of an oligodeoxynucleotide primer. *Proc. Natl. Acad. Sci.* 78: 616.

Stawinski, J., T. Hozumi, S.A. Narang, C.P. Bahl, and R. Wu. 1977. Arylsulfonyltetrazoles, new coupling reagents and further improvements in the triester method for the synthesis of deoxyribooligonucleotides. *Nucleic Acids Res.* 4: 353.

Studencki, A.B. and R.B. Wallace. 1984. Allele-specific hybridization using oligonucleotide probes of very high specific activity: Discrimination of the human β^A- and β^S-globin genes. *DNA* 3: 7.

Suggs, S.V., R.B. Wallace, T. Hirose, E.H. Kawashima, and K. Itakura. 1981a. Use of synthetic oligonucleotides as hybridization probes: Isolation of cloned cDNA sequences for human β_2-microglobulin. *Proc. Natl. Acad. Sci.* 78: 6613.

Suggs, S.V., T. Hirose, T. Miyake, E.H. Kawashima, M.J. Johnson, K. Itakura, and R.B. Wallace. 1981b. Use of synthetic oligodeoxyribonucleotides for the isolation of specific cloned DNA sequences. *ICN-UCLA Symp. Mol. Cell. Biol.* 23: 683.

Takahashi, Y., K. Kato, Y. Hayashizaki. T. Wakabayashi, E. Ohtsuka, S. Matsuki, M. Ikehara, and K. Matsubara.
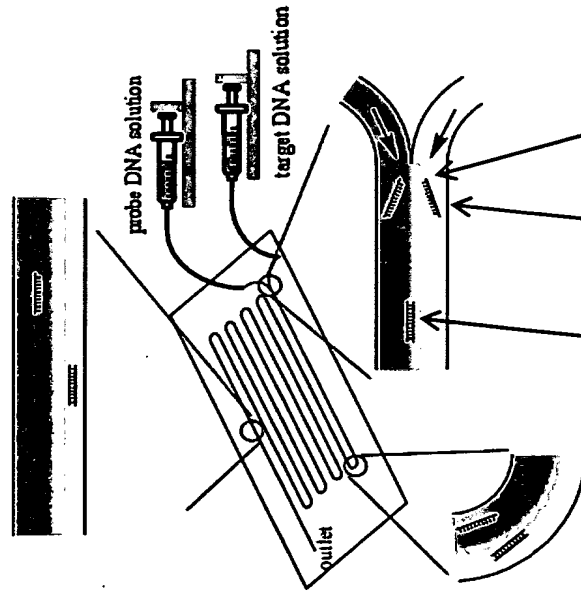
1985. Molecular cloning of the human cholecystokinin gene by use of a synthetic probe containing deoxyinosine. *Proc. Natl. Acad. Sci.* **82:** 1931.

Toole, J.J., J.L. Knopf, J.M. Wozney, L.A. Sultzman, J.L. Buecker, D.D. Pittman, R.J. Kaufman, E. Brown, C. Shoemaker, E.C. Orr, G.W. Amphlett, W.B. Foster, M.L. Coe, G.J. Knutson, D.N. Fass, and R.M. Hewick. 1984. Molecular cloning of a cDNA encoding human antihaemophilic factor. *Nature* **312:** 342.

Uhlenbeck, O.C., F.H. Martin, and P. Doty. 1971. Self-complementary oligoribonucleotides: Effects of helix defects and guanylic acid-cytidylic acid base pairs. *J. Mol. Biol.* **57:** 217.

Ullrich, A., C.H. Berman, T.J. Dull, A. Gray, and J.M. Lee. 1984a. Isolation of the human insulin-like growth factor I gene using a single synthetic DNA probe. *EMBO J.* **3:** 361.

Ullrich, A., A. Gray, A.W. Tam, T. Yang-Feng, M. Tsubokawa, C. Collins, W. Henzel, T. Le Bon, S. Kathuria, E. Chen, S. Jacobs, U. Francke, J. Ramachandran, and Y. Fujita-Yamaguchi. 1986. Insulin-like growth factor I receptor primary structure: Comparison with insulin receptor suggests structural determinants that define functional specificity. *EMBO J.* **5:** 2503.

Ullrich, A., J.R. Bell, E.Y. Chen, R. Herrera, L.M. Petruzzelli, T.J. Dull, A. Gray, L. Coussens, Y.-C. Liao, M. Tsubokawa, A. Mason, P.H. Seeburg, C. Grunfeld, O.M. Rosen, and J. Ramachandran. 1985. Human insulin receptor and its relationship to the tyrosine kinase family of oncogenes. *Nature* **313:** 756.

Ullrich, A., L. Coussens, J.S. Hayflick, T.J. Dull, A. Gray, A.W. Tam, J. Lee, Y. Yarden, T.A. Libermann, J. Schlessinger, J. Downward, E.L.V. Mayes, N. Whittle, M.D. Waterfield, and P.H.

Seeburg. 1984b. Human epidermal growth factor receptor cDNA sequence and aberrant expression of the amplified gene in A431 epidermoid carcinoma cells. *Nature* **309:** 418.

Wahls, W.P. and M. Kingzette. 1988. No runs, no drips, no errors: A new technique for sealing polyacrylamide gel electrophoresis apparatus. *BioTechniques* **6:** 308.

Wallace, R.B., M.J. Johnson, T. Hirose, T. Miyake, E.H. Kawashima, and K. Itakura. 1981. The use of synthetic oligonucleotides as hybridization probes. II. Hybridization of oligonucleotides of mixed sequence to rabbit β-globin DNA. *Nucleic Acids Res.* **9:** 879.

Wood, W.I., J. Gitschier, L.A. Lasky, and R.M. Lawn. 1985. Base composition-independent hybridization in tetramethylammonium chloride: A method for oligonucleotide screening of highly complex gene libraries. *Proc. Natl. Acad. Sci.* **82:** 1585.

Wood, W.I., D.J. Capon, C.C. Simonsen, D.L. Eaton, J. Gitschier, B. Keyt, P.H. Seeburg, D.H. Smith, P. Hollingshead, K.L. Wion, E. Delwart, E.G.D. Tuddenham, G.A. Vehar, and R.M. Lawn. 1984. Expression of active human factor VIII from recombinant DNA clones. *Nature* **312:** 330.

Wozney, J.M. 1989. Using a purified protein to clone its gene. *Methods Enzymol.* (in press).

Wu, R. 1972. Nucleotide sequence analysis of DNA. *Nature New Biol.* **236:** 198.

Zassenhaus, H.P., R.A. Butow, and Y.P. Hannon. 1982. Rapid electroelution of nucleic acids from agarose and acrylamide gels. *Anal. Biochem.* **125:** 125.

Zoller, M.J. and M. Smith. 1984. Oligonucleotide-directed mutagenesis: A simple method using two oligonucleotide primers and a single-stranded DNA template. *DNA* **3:** 479.
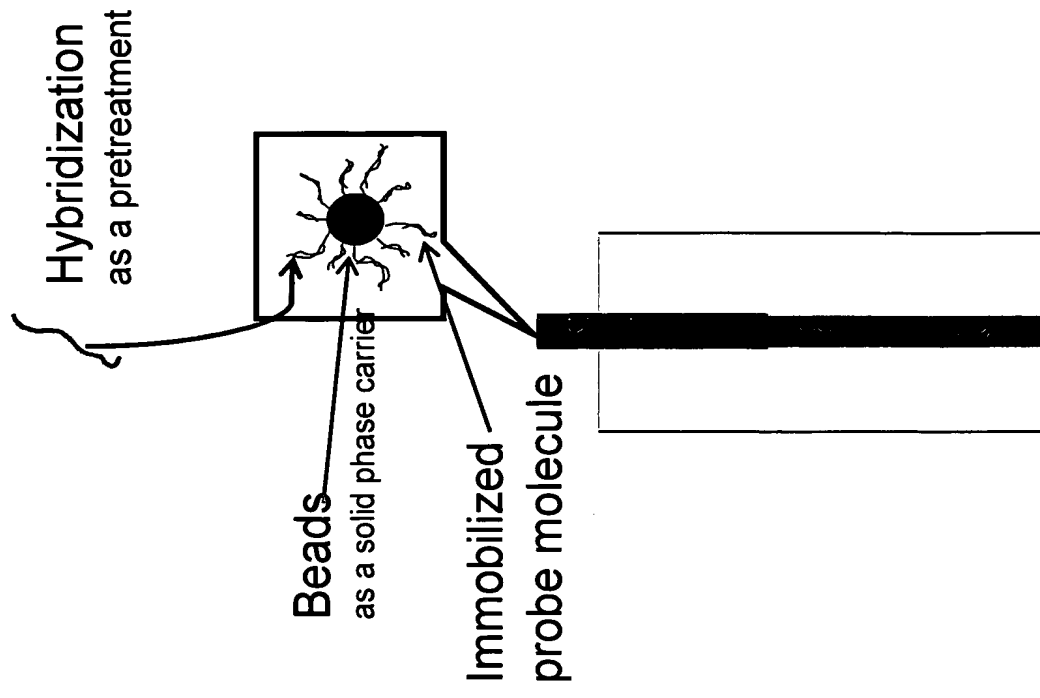
Flow cytometry

Hybridization
as a pretreatment

Beads
as a solid phase carrier

Immobilized
probe molecule

Our method

probe DNA solution

target DNA solution

outlet

On-flow
hybridization

Without solid phase carrier

Non-immobilized probe molecule

3-D Simulation and Visualization of Laminar Flow in a Microchannel with Hair-Pin Curves

Y. Yamaguchi, F. Takagi, K. Yamashita, H. Nakamura, and H. Maeda
National Institute of Advanced Industrial Science and Technology, Tosu 841-0052, Japan

K. Sotowa and K. Kusakabe
Dept. of Applied Chemistry, Kyushu University, Fukuoka 812-8581, Japan

Y. Yamasaki and S. Morooka
Dept. of Chemical Engineering, Fukuoka University, Fukuoka 814-0180, Japan

The purpose of the present study was to investigate fluidic behavior in a microchannel with hair-pin curves, using a three-dimensional (3-D) computational fluid dynamics simulation, and to observe the 3-D flow pattern, to validate the simulation. The microchannel used was fabricated on a PMMA plate using a flat-end mill. The channel width and depth were 210 and 205 μm, respectively, and the radius of each hair-pin curve was 500 μm. Two liquids; purified water and an aqueous solution of 50 μmol/L fluorescein, were introduced into the microchannel through different inlets and were merged, forming a side-by-side parallel flow in the straight channel. When the average velocity was 25 mm/s, the liquid was thrust outward by centrifugal force and, as a result, the vertical line that crossed the central axis was distorted after passing the first hair-pin curve. At the second hair-pin curve, the centrifugal force was exerted in the opposite direction, and the distorted line returned nearly to an initial vertical line. When the average velocity was 125 mm/s, however, the vertical line, which was distorted at the first hair-pin curve, did not recover to the initial vertical line after the second curve. The interface between the two liquids was permanently waved. The simulation was in good agreement with the experimental data. The results suggest that the diffusion rate through the interface of two liquids in microchannels with hair-pin curves can increase, compared to that in straight microchannels. © 2004 American Institute of Chemical Engineers *AIChE J*, 50: 1530–1535, 2004
Keywords: microfluidics, confocal fluorescence microscopy, computational fluid dynamics, microchannel, microreactor

Introduction

Miniaturized devices for use in chemical analysis and material synthesis have attracted considerable interest in

recent years (Ehrfeld, 2000). These devices usually contain microchannels, the widths of which are 1–1000 μm. Such narrow channels provide unique reaction fields, basically because the outside surface area per unit reactor volume is large in comparison with conventional reactors. Examples of such applications include: the selective synthesis of organic compounds using organic and aqueous phases (Hisamoto et al., 2001), the enzyme reaction with

Attachment D
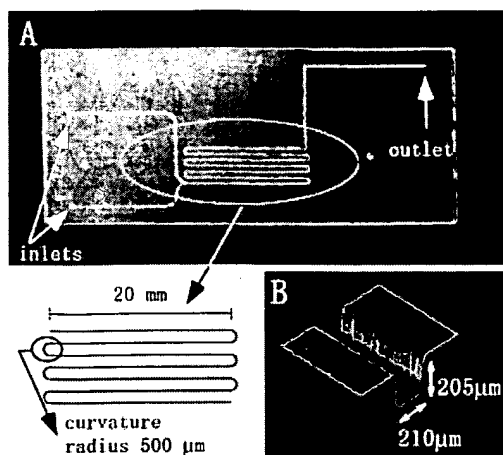
Figure 1. Fabrication of a microchannel. A: top view, B: details of the channel.

high yields (Kanno et al., 2001; Miyazaki et al., 2001), and the synthesis of nanoparticles with well-controlled sizes (Nakamura et al., 2002). When particles that are lighter or heavier than the liquid are suspended in a microchannel with sharp corners, a centrifugal force is induced. As a result, the path lines of the particles deviate from the path lines of the liquid stream. The same effect would be expected when two liquids with different densities are introduced into microchannels.

For liquid-phase systems in microchannels, the diffusion rate is a key factor in controlling reaction rates. Because the flow is laminar, the diffusion rate between the two liquids is dependent on the contact area. We recently reported on some two-dimensional (2-D) observations of flow characteristics in a microchannel (width = 210 μm, depth = 205 μm) with hair-pin corners (Kawazumi et al., 2002). Red- and green-colored water with the same density were introduced into the microchannel in a side-by-side parallel flow mode, and the flow pattern was observed from the vertical direction using a color CCD camera with a 200× magnifying lens. The color of the microchannel flow changed before and after the hair-pin corner. This was caused by a local circulating flow, induced by a centrifugal force acting on the homogeneous liquid. The interface area and, as a result, the diffusion between the two liquids could be influenced by this secondary flow. However, the flow was observed only from the vertical direction, and we were not able to elucidate the three-dimensional (3-D) behavior of the liquids.

The purpose of the present study is to demonstrate microfluidic behavior using 3-D computational fluid dynamics simulation, and to validate the simulation by observing the 3-D hydrodynamic behavior. At the macro level, fluidic simulation and visualization have been extensively performed, and the secondary flow induced at a corner has been analyzed (Cheng et al., 1976; Ghia and Sokhey, 1977). At the micro level, however, research on 3-D flow visualization has been only recently begun. Wang et al. (1995) used small beads as the tracer, but these beads might disturb the flow in a microspace. Manz et al. (1995) measured the

velocity distribution in a capillary using an NMR micro-imaging technique, but the spatial resolution was larger than 10 μm, which was not sufficiently small for measurements in microchannels. In contrast, a measurement technique using single-molecule fluorescein, coupled with fluorescence confocal microscopy, was recently developed and permitted a description of flow with a spatial resolution as small as 1 μm (Gösch et al., 2000; Ismagilov et al., 2000). We directed our attention to applying this principle to observations of the cross-sectional plane of fluids in microchannels and to clarify the interface configuration. An understanding of the flow dynamics would be highly desirable for designing chemical reactions at the interface of solutions (Kenis et al., 1999; Zhao et al., 2002), as well as extraction between aqueous and organic phases (Hisamoto et al., 2001), and, furthermore, in elucidating the origin of much higher chemical reaction yields in microchannel reactors, compared to those in well-mixed batch reactors (Kanno et al., 2001; Miyazaki et al., 2001; Tanaka et al., 2001).

Experimental Studies

A microchannel was fabricated mechanically on a PMMA plate (Kawazumi et al., 2002), using a Robodrill (FANUC, Oshino-mura, Japan) with a flat-end mill (diameter = 200 μm, Hitachi Power Tools, Osaka, Japan). Figure 1a shows a complete view of the microchannel used, and Figure 1b shows the details of the channel. The channel width and depth were 210 and 205 μm, respectively. The radius of each hair-pin curve was 500 μm, unless otherwise stated. The wall roughness was determined to be less than 5% of the depth, as evidenced by a laser microscope measurement. After fabrication, the channel plate was covered with a plat top plate and sealed by heating. Programmable syringe pumps were connected to the inlets by Teflon tubing.

Two liquids were prepared: purified water and an aqueous solution of 50 μmol/L fluorescein. The densities were practically the same. The two liquids were introduced into the microchannel through different inlets and were merged to form a side-by-side parallel flow in the straight channel. A confocal fluorescence microscopy system (Nikon, Tokyo,
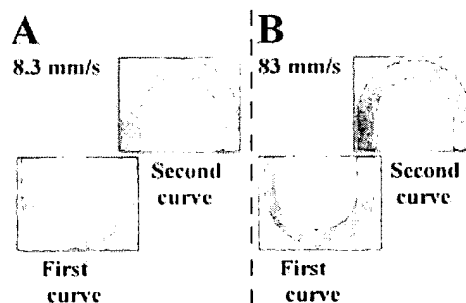
Figure 2. Two-dimensional observation of flow using red- and green-colored water. Two liquids are introduced into the channel in a side-by-side parallel flow configuration.
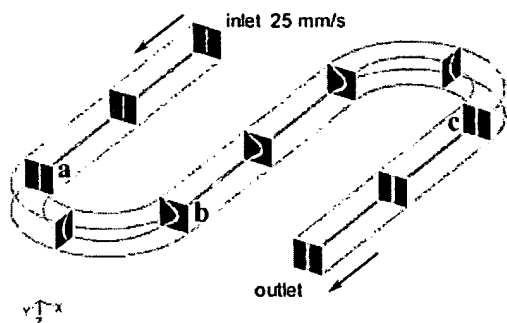
Figure 3. Distortion of the initially vertical line during its passage through the microchannel (simulation). Average velocity = 25 mm/s.
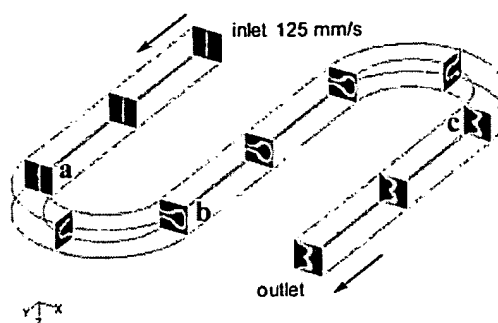

Figure 5. Distortion of the initially vertical line during its passage through the microchannel (simulation). Average velocity = 125 mm/s.

Japan) was used for the measurement. An Ar laser (wavelength = 488 nm, output = 25 mW) was scanned through an objective lens (ELWD-20x) in a 3-D manner, and the fluorescence emission from the fluorescein solution was detected at a resolution of about 3 μm. To observe the 2-D flow pattern, samples of red- and green-colored water were also used. The color change in the microchannel flow was recorded through the upper cover plate.

Computational Fluid Dynamics Simulation

The dimensions of the microchannel used for the simulation are assumed to be: width = depth = 200 μm, straight channel length = 20 mm, and curvature radius = 500 μm. Three-dimensional simulations were carried out using FLUENT 6.0 (Fluent USA, Lebanon, NH) based on a finite-volume scheme. The Euler mixing model, suitable for mutually miscible fluids, was adopted. Molecules of the liquid microscopically slip on the channel wall (Thompson and Trolan, 1997). For simplicity, however, no slip conditions were assumed in the present study (Barrat and Bocquet, 1999; Stroock et al., 2002). The inlet plane was divided in 40 × 40 mesh sections, and the total number of mesh

sections in the calculated space was 475,200. A computation with nearly double the number of mesh sections gave approximately the same results. An iterative calculation for solving the Navier–Stokes equations was carried out with the second-order accuracy for pressure, and the SIMPLE algorithm was used for pressure–velocity coupling.

Results and Discussion

Figure 2 shows a 2-D observation of the flow pattern, using the red- and green-colored waters. When the average velocity is 8.3 mm/s, the two liquids form a side-by-side parallel flow, and no color change is observed in the microchannel. When the average flow velocity is increased to 83 mm/s, however, the outside red region overrides the inside green region after the first hair-pin curve, and the color of the flow changes to red. After passing the second turn with an opposite curvature, a green liquid emerges, and the flow pattern returns to the original side-by-side parallel flow.

Figure 3 shows the result of the simulation at an average velocity of 25 mm/s. The velocity along the central axis is
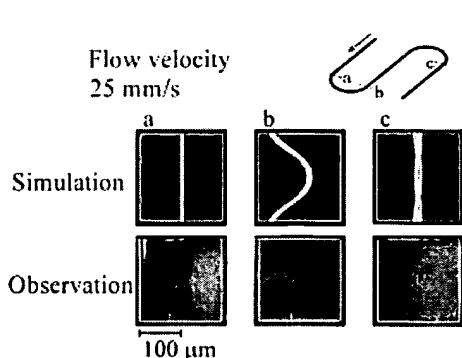

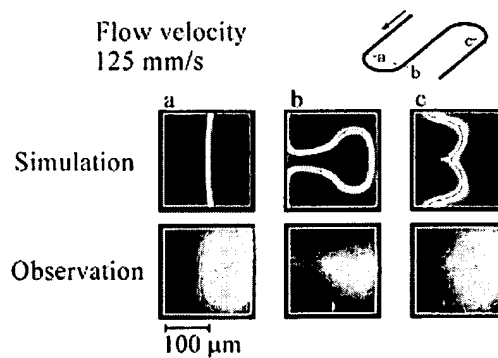**Figure 4. Comparison between simulation and experiment for 3-D flow patterns. Average velocity = 25 mm/s.**

Figure 6. Comparison between simulation and experiment for 3-D flow patterns. Average velocity = 125 mm/s.
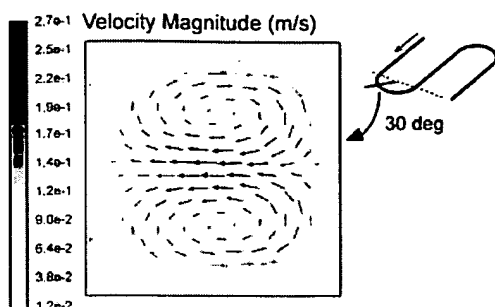
Figure 7. Velocity distribution of the secondary flow at the first turn. Average velocity = 125 mm/s.

the largest and is the most strongly affected by the centrifugal force. As a result, the liquid flowing along the central axis is thrust outward the most vigorously. Thus, the vertical line that crosses the central axis is distorted after the first-turn. After the second turn, the centrifugal force is exerted in the opposite direction, and the distorted line returns nearly to the initial vertical line.

Figure 4 shows a comparison between the simulation and the experimental results for the vertical cross-sectional plane under the same conditions as were used in Figure 3. The average liquid velocity is 25 mm/s. The upper and lower pictures a, b, and c correspond to the situations before the first turn, after the first turn, and after the second turn, respectively. The lines in the upper pictures, calculated by the simulation, indicate a boundary between the water and the fluorescein solution. The fluorescein solution, which initially flows on the right-hand side in this cross section, is thrust outward after the first turn and then returns to the initial position after the second turn. The simulation is in good agreement with the experimental data.

Figure 5 shows the results of the simulation and an observation for the case where the average velocity is 125 mm/s. The vertical line observed in the initial straight channel is heavily distorted after the first turn. After the second turn, the two liquid flows largely return to the original positions, and the side-by-side parallel flow pattern is again observed. In contrast with the result for a velocity of 25 mm/s, however, the distorted line is not fully recovered to the initial vertical line after the second turn. The interface between the two liquids is permanently distorted by the stronger centrifugal force. Figure 6 shows a comparison between simulation and observation at a velocity of 125 mm/s. The upper pictures show the calculated interfaces, and the lower pictures show the results of the 3-D observation. The upper and lower pictures agree well, as was found for a velocity of 25 mm/s.

Figure 7 shows the velocity distribution on the vertical plane perpendicular to the main liquid flow at the middle point of the first turn. The liquid at the outer periphery is forced outward, and the liquid at the upper and lower periphery moves inward to compensate for the outward flow. This secondary flow perturbs the interface configuration. These results are in agreement with findings for laminar flow

at the macro level (Cheng et al., 1976; Ghia and Sokhey, 1977). The flow in a curved channel is expressed by the Dean number

$$k = \mathrm{Re}\,\sqrt{a/R} \qquad (1)$$

where Re is the Reynolds number, a is the channel radius, and R is the curvature radius. A single vortex pair appears in the region of $K < 140$ (Ghia and Sokhey, 1977). The value of the Dean number in the present study is less than 20, which supports the formation of secondary flows in the microchannel.

Liquid-phase chemical reactions and material syntheses in 3-D microspaces are substantially influenced by diffusion across the interface. The degree of diffusion is expressed by the parameter P_Z

$$P_Z = \frac{Dt}{L^2} \qquad (2)$$

where D is the diffusion coefficient, t is the time of diffusion, and L is the representative length of the space. The representative length can be defined by

$$L = 6V/S \qquad (3)$$

where V is the volume and S the interfacial area through which diffusion occurs (Crank, 1975). In a microchannel with hair-pin curves, the interface of the two liquids is not a simple flat plane, as seen in Figures 4 and 6. Figure 8 summarizes the interface configurations as functions of average velocity and curvature radius. Data for hair-pin curves with a curvature radius of 250 μm are included in this figure. The interfacial area per unit length of the microchannel increases to αS_0, where S_0 is the flat interfacial area and α ($=S/S_0$) is a coefficient larger than unity. Parameter P_Z is inversely proportional to L^2, indicating that the time required for diffusion decreases with an increase in $(\alpha S_0)^2$. As shown in Figure 8, α exceeds 3 in some cases. This suggests that the diffusion rate through the interface of the two liquids in microchannels with hair-pin curves greatly increases in comparison with that in straight microchannels. Because the two liquids used in this study are miscible, the interface of the liquids disappears after passing a certain number of hair-pin curves. In some cases, reaction rates may be strongly affected by the manner in which aqueous solutions are fed and mixed in microchannels (Kanno et al., 2001; Miyazaki et al., 2001; Tanaka et al., 2001). A further study of the role of microchannel curvature is currently under way.

Figure 8. Effects of curvature diameter and average velocity on flow patterns and interface configurations in the microchannel.

Conclusions

Three-dimensional computational fluid dynamics simulations were performed, with respect to the fluidic behavior of laminar liquid flows in microchannels with hair-pin curves. The simulation results were validated by 3-D observation by confocal fluorescence microscopy. These results revealed that the interface configuration of two liquids was affected by secondary flow, induced by centrifugal force at the corners. The increased interface area of two laminar liquids could promote a mass transfer based on diffusion. The success of chemical reactions and material syntheses inside microchannels is often dependent on flow properties, and higher yields are obtained, compared to reactions in well-mixed reactors. The results obtained in this study suggest the importance of microchannel design based on a 3-D comprehension of the fluid and accompanying mixing behavior.

Acknowledgments

Literature Cited

Barrat, J.-L., and L. Bocquet, "Influence of Wetting Properties on Hydrodynamic Boundary Conditions at a Fluid/Solid Interface," *Faraday Discuss.*, 112, 119 (1999).

Cheng, K. C., R.-C. Lin, and J.-W. Ou, "Fully Developed Laminar Flow in Curved Rectangular Channels," *Trans ASME: Ser. I*, 98(1), 41 (1976).

Crank, J., *The Mathematics of Diffusion*, 2nd ed., Clarendon Press, Oxford, UK (1975).

Ehrfeld, W., *Microreaction Technology: Industrial Prospects*, Springer-Verlag, Berlin (2000).

Ghia, K. N., and J. S. Sokhey, "Laminar Incompressible Viscous Flow in Curved Ducts of Regular Cross Sections," *Trans. ASME: Ser. I*, 99(4), 640 (1977).

Gösch, M., H. Blom, J. Holm, T. Heino, and R. Rigler, "Hydrodynamic Flow Profiling in Microchannel Structures by Single Molecule Fluorescence Correlation Spectroscopy," *Anal. Chem.*, 72(14), 3260 (2000).

Hisamoto, H., T. Saito, M. Tokeshi, A. Hibara, and T. Kitamori, "Fast and High Conversion Phase-Transfer Synthesis Exploiting the Liquid–Liquid Interface Formed in a Microchannel Chip," *Chem. Commun.*, 24, 2662 (2001).

Ismagilov, R. F., A. D. Stroock, P. J. A. Kenis, G. Whitesides, and H. A. Stone, "Experimental and Theoretical Scaling Laws for Transverse Diffusive Broadening in Two-Phase Laminar Flows in Microchannels," *Appl. Phys. Lett.*, 76(17), 2376 (2000).

Kanno, K., H. Maeda, S. Izumo, M. Ikuno, K. Takeshita, A. Tashiro, and M. Fujii, "Rapid Enzymatic Transglycosylation and Oligosaccharide Synthesis in a Microchip Reactor," *Lab on a Chip*, 2(1), 15 (2002).

Kawazumi, H., A. Tashiro, K. Ogino, and H. Maeda, "Observation of Fluidic Behavior in a Polymethylmethacrylate-Fabricated Microchannel by a Simple Spectroscopic Analysis," *Lab on a Chip*, 2(1), 8 (2002).

Kenis, P. J. A., R. F. Ismagilov, and G. M. Whitesides, "Microfabrication Inside Capillaries Using Multiphase Laminar Flow Patterning," *Science*, 285(5424), 83 (1999).

Manz, B., P. Stilbs, B. Jönsson, O. Söderman, and P. T. Callaghan, "NMR Imaging of the Time Evolution of Electroosmotic Flow in a Capillary," *J. Phys. Chem.*, 99(29), 11297 (1995).

Miyazaki, M., H. Nakamura, and H. Maeda, "Improved Yield of Enzyme Reaction in Microchannel Reactor," *Chem. Lett.*, 5, 442 (2001).

Nakamura, H., Y. Yamaguchi, M. Miyazaki, M. Uehara, H. Maeda, and P. Mulvaney, "Continuous Preparation of CdSe Nanocrystals by a Microreactor," *Chem. Lett.*, 10, 1072 (2002).

Stroock, A. D., S. K. Dertinger, G. M. Whitesides, and A. Ajdari, "Patterning Flows Using Grooved Surfaces," *Anal. Chem.*, 74(20), 5306 (2002).

Tanaka, Y., M. N. Slyadnev, K. Sato, M. Tokeshi, H.-B. Kim, and T. Kitamori, "Acceleration of an Enzymatic Reaction in a Microchip," *Anal. Sci.*, **17**(7), 809 (2001).

Thompson, P. A., and S. M. Troian, "A General Boundary Condition for Liquid Flow at Solid Surfaces," *Letters to Nature*, **389**(6649), 360 (1997).

Wang, W., Y. Liu, G. J. Sonek, M. W. Berns, and R. A. Keller, "Optical Trapping and Fluorescence Detection in Laminar Flow Streams," *Appl. Phys. Lett.*, **67**(8), 1057 (1995).

Zhao, B., N. O. L. Viernes, J. S. Moore, and D. J. Beebe, "Control and Applications of Immiscible Liquids in Microchannels," *J. Am. Chem. Soc.*, **124**(19), 5284 (2002).